



NAVAL POSTGRADUATE SCHOOL

MONTEREY, CALIFORNIA

THESIS

**APPLICATION OF THIN FILM PHOTOVOLTAIC CIGS
CELLS TO EXTEND THE ENDURANCE OF SMALL
UNMANNED AERIAL SYSTEMS**

by

Matthew D. Lai

June 2017

Thesis Advisor:
Second Reader:

Sherif Michael
James Calusdian

Approved for public release. Distribution is unlimited.

THIS PAGE INTENTIONALLY LEFT BLANK

REPORT DOCUMENTATION PAGE			<i>Form Approved OMB No. 0704-0188</i>	
Public reporting burden for this collection of information is estimated to average 1 hour per response, including the time for reviewing instruction, searching existing data sources, gathering and maintaining the data needed, and completing and reviewing the collection of information. Send comments regarding this burden estimate or any other aspect of this collection of information, including suggestions for reducing this burden, to Washington headquarters Services, Directorate for Information Operations and Reports, 1215 Jefferson Davis Highway, Suite 1204, Arlington, VA 22202-4302, and to the Office of Management and Budget, Paperwork Reduction Project (0704-0188) Washington, DC 20503.				
1. AGENCY USE ONLY (Leave blank)		2. REPORT DATE June 2017		3. REPORT TYPE AND DATES COVERED Master's thesis
4. TITLE AND SUBTITLE APPLICATION OF THIN FILM PHOTOVOLTAIC CIGS CELLS TO EXTEND THE ENDURANCE OF SMALL UNMANNED AERIAL SYSTEMS			5. FUNDING NUMBERS	
6. AUTHOR(S) Matthew D. Lai				
7. PERFORMING ORGANIZATION NAME(S) AND ADDRESS(ES) Naval Postgraduate School Monterey, CA 93943-5000			8. PERFORMING ORGANIZATION REPORT NUMBER	
9. SPONSORING /MONITORING AGENCY NAME(S) AND ADDRESS(ES) N/A			10. SPONSORING / MONITORING AGENCY REPORT NUMBER	
11. SUPPLEMENTARY NOTES The views expressed in this thesis are those of the author and do not reflect the official policy or position of the Department of Defense or the U.S. Government. IRB number ____N/A____.				
12a. DISTRIBUTION / AVAILABILITY STATEMENT Approved for public release. Distribution is unlimited.			12b. DISTRIBUTION CODE	
13. ABSTRACT (maximum 200 words) Vulnerability and unknowns are characteristic in all military missions. With an end goal to enhance situational awareness and provide the military unit an advantage, small unmanned aerial systems (SUAS) have been utilized to provide surveillance and reconnaissance information. A noteworthy restriction of SUAS is the constrained flight endurance due to their limited onboard battery capacity. Currently, most military SUAS are dependent on their onboard battery supply, which limits flight time to about 60 to 200 minutes before the vehicle must land for replacement/recharge of its battery. The integration of photovoltaic (PV) cells onto SUAS has been proven to extend their flight endurance. In this project, we extended the flight endurance by supplementing the onboard battery with encapsulated copper-indium-gallium di-selenide (CIGS) thin-film photovoltaic (TFPV) cells. The completely incorporated framework was tentatively tested to demonstrate the practicality and constraints of supplementing the onboard battery source with a PV array. Due to our limited access to the Puma unmanned aerial vehicle (UAV), our estimate of the Puma's extended flight endurance with PV array is hypothesized based on its operational manual and the operating experience of the Evolving Resources Incorporated (ERI). On that basis, we conclude that the inclusion of the CIGS TFPV cells theoretically exceeds the power consumption of the Puma UAV. The Puma's estimated flight time endurance is dramatically increased, creating an indefinite day flight time under ideal sunny conditions as compared to its original 200 minutes. We recommend further study and testing of the integration of CIGS TFPV cells with the Puma UAV or other Group 1 SUAS.				
14. SUBJECT TERMS photovoltaics, thin film photovoltaics, solar, unmanned aerial vehicle, small unmanned aircraft systems, situational awareness, intelligence, surveillance, reconnaissance, Puma RQ-20B DDL			15. NUMBER OF PAGES 53	
			16. PRICE CODE	
17. SECURITY CLASSIFICATION OF REPORT Unclassified	18. SECURITY CLASSIFICATION OF THIS PAGE Unclassified	19. SECURITY CLASSIFICATION OF ABSTRACT Unclassified	20. LIMITATION OF ABSTRACT UU	

THIS PAGE INTENTIONALLY LEFT BLANK

Approved for public release. Distribution is unlimited.

**APPLICATION OF THIN FILM PHOTOVOLTAIC CIGS CELLS TO EXTEND
THE ENDURANCE OF SMALL UNMANNED AERIAL SYSTEMS**

Matthew D. Lai
Lieutenant, United States Navy
B.S., University of Washington, 2009

Submitted in partial fulfillment of the
requirements for the degree of

MASTER OF SCIENCE IN ELECTRICAL ENGINEERING

from the

**NAVAL POSTGRADUATE SCHOOL
June 2017**

Approved by: Sherif Michael
Thesis Advisor

James Calusdian
Second Reader

R. Clark Robertson
Chair, Department of Electrical and Computer Engineering

THIS PAGE INTENTIONALLY LEFT BLANK

ABSTRACT

Vulnerability and unknowns are characteristic in all military missions. With an end goal to enhance situational awareness and provide the military unit an advantage, small unmanned aerial systems (SUAS) have been utilized to provide surveillance and reconnaissance information. A noteworthy restriction of SUAS is the constrained flight endurance due to their limited onboard battery capacity. Currently, most military SUAS are dependent on their onboard battery supply, which limits flight time to about 60 to 200 minutes before the vehicle must land for replacement/recharge of its battery. The integration of photovoltaic (PV) cells onto SUAS has been proven to extend their flight endurance. In this project, we extended the flight endurance by supplementing the onboard battery with encapsulated copper-indium-gallium di-selenide (CIGS) thin-film photovoltaic (TFPV) cells. The completely incorporated framework was tentatively tested to demonstrate the practicality and constraints of supplementing the onboard battery source with a PV array. Due to our limited access to the Puma unmanned aerial vehicle (UAV), our estimate of the Puma's extended flight endurance with PV array is hypothesized based on its operational manual and the operating experience of the Evolving Resources Incorporated (ERI). On that basis, we conclude that the inclusion of the CIGS TFPV cells theoretically exceeds the power consumption of the Puma UAV. The Puma's estimated flight time endurance is dramatically increased, creating an indefinite day flight time under ideal sunny conditions as compared to its original 200 minutes. We recommend further study and testing of the integration of CIGS TFPV cells with the Puma UAV or other Group 1 SUAS.

THIS PAGE INTENTIONALLY LEFT BLANK

TABLE OF CONTENTS

I.	INTRODUCTION.....	1
A.	BACKGROUND	1
B.	SUAS CAPABILITIES AND MISSIONS	3
C.	OBJECTIVE	3
D.	APPROACH.....	4
II.	FUNDAMENTALS.....	5
A.	UNMANNED AERIAL VEHICLES.....	5
1.	PUMA AE (RQ-20B)	6
2.	RAVEN (RQ-11B).....	8
3.	WASP AE (RQ-12A).....	9
4.	DESERT HAWK III.....	10
B.	PRACTICAL SOLAR CELLS.....	11
1.	FACTORS THAT INFLUENCE SOLAR EFFICIENCY	12
2.	ENCAPSULATED FLEXIBLE TFPV CELLS	14
III.	TFPV ON PUMA	17
A.	BEST SUAS FOR SOLAR CELL INTEGRATION	17
B.	GLOBAL SOLAR TFPV SOLAR ARRAY.....	19
IV.	EXPERIMENTAL RESULTS.....	21
A.	FG-SM12-11 SOLAR MODULE TESTING.....	21
B.	LEFT AND RIGHT TFPV SOLAR ARRAY	22
C.	FULL SOLAR ARRAY.....	25
D.	PV EFFICIENCY AND FILL FACTOR	27
E.	SUMMARY	28
V.	CONCLUSION AND RECOMMENDATIONS.....	29
A.	SUMMARY	29
B.	FUTURE WORK.....	30
1.	Obtaining the Full Puma AV for Testing	30
2.	Testing Other Group 1 AVs with TFPV cells.....	30
3.	Utilize MPPTs in Design.....	30
4.	Further Study of the Puma's Smart Battery	31
5.	Development of Solar Battery Charger	31
	LIST OF REFERENCES	33
	INITIAL DISTRIBUTION LIST	35

THIS PAGE INTENTIONALLY LEFT BLANK

LIST OF FIGURES

Figure 1.	Puma AE (RQ-20B). Source: [5].	6
Figure 2.	Raven (RQ-11B). Source: [9].	8
Figure 3.	Wasp AE (RQ-12A). Source: [10].	10
Figure 4.	IV Curve Example at Different Solar Intensity. Adapted from [2].	12
Figure 5.	Example of How Temperature Affect a Single Solar Cell. Source: [15].	13
Figure 6.	NREL Best Research-Cell Efficiencies, since 1976. Source: [16].	14
Figure 7.	Schematic Illustration of a Typical CIGS Substrate. Source: [17].	15
Figure 8.	Puma Li-ion Polymer Battery. Source: [18].	18
Figure 9.	Puma Wing.	19
Figure 10.	Global Solar FG-SM12-11 Submodule Typical Performance. Adapted from [19].	20
Figure 11.	Average IV and Power Curve of a Single TFPV Submodule.	22
Figure 12.	Un-Trimmed Submodule (left), and Trimmed Submodule (right)	23
Figure 13.	Average IV and Power Curve for Left and Right Array	24
Figure 14.	Male and Female DC Power Supply Connectors	25
Figure 15.	Fully Assembled Wing with the Solar Arrays	26
Figure 16.	Average IV and Power Curve for Combined Solar Arrays	26

THIS PAGE INTENTIONALLY LEFT BLANK

LIST OF TABLES

Table 1.	NATO UAV Classification. Source: [1].	2
Table 2.	UAV Classifications. Source: [4].	5
Table 3.	Puma AE (RQ-20B) Specifications. Source: [5].	7
Table 4.	Raven (RQ-11B) Specifications. Source: [9].	9
Table 5.	Wasp AE (RQ-12A) Specifications. Source: [10].	10
Table 6.	Desert Hawk III Specifications. Adapted from [13].	11
Table 7.	Global Solar FG-SM12-11 TFPV Cell Specifications. Adapted from [19].	20
Table 8.	Electrical Characteristics of a Single TFPV Submodule	21
Table 9.	Left and Right Solar Array Electrical Characteristics	24
Table 10.	Combined Solar Electrical Characteristics	26

THIS PAGE INTENTIONALLY LEFT BLANK

LIST OF ACRONYMS AND ABBREVIATIONS

AE	all environment
AV	air vehicle
ARC	antireflective coating
CdS	cadmium sulfide
CIGS	copper-indium-gallium di-selenide
COTS	commercial-off-the-shelf
DC	direct current
DDL	digital data link
DOD	Department of Defense
ERI	Evolving Resources Incorporated
GCS	ground control station
GPS	Global Positioning System
IBC	interdigitated back contact
IR	infrared
ISC	short-circuit current
ISR	intelligence, surveillance, and reconnaissance
IV	current-voltage
Li-ion	lithium ion
Mo	molybdenum
MP	maximum power
MPPT	maximum power point tracker
NATO	North Atlantic Treaty Organization
PV	photovoltaic
RSTA	reconnaissance, surveillance, and target acquisition
SUAS	small unmanned aircraft systems
STC	standard test conditions
TFPV	thin-film photovoltaic
UAV	unmanned aerial vehicle
VOC	open-circuit voltage

THIS PAGE INTENTIONALLY LEFT BLANK

ACKNOWLEDGMENTS

I would like to thank everyone in the Solar Puma project, especially my thesis advisor, Dr. Sherif Michael, and my second reader, Dr. James Calusdian. Without their help and devotion, this venture couldn't have been finished. I would also like to thank Danny Ensenat, Ryan Shero, Richard Gomez, and Albert Gomez at Evolving Resources Incorporated for allowing us access to their Puma drones, giving us a Puma wing for our testing, and allowing us to gather actual flight and battery data. Finally, and most importantly, I would like to thank my wife, Mary Grace, as well as our two children, Lleyton and Llayza. Without their steady guidance, inspiration, understanding, and support of my research, none of this would have been possible.

THIS PAGE INTENTIONALLY LEFT BLANK

I. INTRODUCTION

A. BACKGROUND

Unmanned Aerial Vehicles (UAVs) have been widely utilized in all branches of the U.S. military. The use of UAV systems has been effective in providing critical mission utility in observation, reconnaissance, surveillance, and target identification. The main advantage of utilizing UAVs is that they can be operated without an onboard pilot, reducing the risk of losing a service member behind enemy lines. Another advantage of using UAVs is their cost; a UAV does not require the extra equipment for manned aircraft, translating to a reduction in weight, size, and complexity of the aircraft. After initial procurement costs, operational expenses are reduced, and it is quicker to train UAV operators than to train pilots. Another advantage to using UAVs is the fatigue factor; pilots are human, they have to land to get rest, while UAV operators have the option to relieve one another while the aircraft remains on station.

This applies to all types of surveillance and reconnaissance UAV systems. To help in surveillance operations, threat assessments and mission planning can be concentrated preceding a mission by means of stationary satellite imaging or airborne photography. Nonetheless, while stationary imaging is more successful than scouting parties as regards observation, it is constrained in that pictures may not mirror the present circumstance, contingent upon the measure of time that passes before accumulated pictures are prepared.

The North Atlantic Treaty Organization (NATO) classifies UAVs by their normal employment [1]. NATO's Class I are the tactical man-portable UAVs, Class II are the tactical mid-range UAVs, and Class III are the strategic long-range UAVs [1]. Details of these NATO UAV classifications are shown in Table 1. Relating to this thesis, we concentrated on expanding the flight endurance of the Puma UAV, which is in the Class I category.

Table 1. NATO UAV Classification. Source: [1].

NATO Classification					
Class & Weight, w (kg)	Category & Weight, w (kg)	Normal Employment	Normal Operating Altitude, h (ft)	Normal Mission Radius (km)	Example Platform
Class I w < 150	Small w > 20 kg	Tactical Unit (employs launch system)	$h \leq 5000$ AGL	50 (LOS)	Luna, Hermes 90
	Mini $2 \leq w \leq 20$ kg	Tactical Unit (manual launch)	$h \leq 3000$ AGL	25 (LOS)	ScanEagle, Skylark, Raven, DH3, Aladin, Strix
	Micro w < 2	Tactical Patrol/section, Individual (single operator)	$h \leq 200$ AGL	5 (LOS)	Black Widow
Class II $150 \leq w \leq 600$	Tactical	Tactical Formation	$h \leq 10,000$ AGL	200 (LOS)	Sperwer, Iview 250, Hermes 450, Aerostar, Ranger
Class III w > 600	Strike/Combat	Strategic/National	$h \leq 65,000$	Unlimited (BLOS)	
	HALE	Strategic/National	$h \leq 65,000$	Unlimited (BLOS)	Global Hawk
	MALE	Operational/Theater	$h \leq 45,000$ MSL	Unlimited (BLOS)	Predator A, Predator B, Heron, Heron TP, Hermes 900

Small UAVs are consistently utilized at all levels of the military. Their portability provides quick assembly/disassembly and launch for intelligence, surveillance, and reconnaissance (ISR) missions. The main limitations of small unmanned aerial system (SUAS) are their flight endurance, which is restricted by their onboard battery supply. Their endurance is normally restricted to between 60 and 200 minutes, after which the SUAS must be recovered for battery replacement or battery recharge. If the operator decides to re-launch that same SUAS for any mission, the same pre-flight test procedures must be conducted in accordance with the operational manual prior to operating the SUAS. In total, that is a loss of about 30–45 minutes between recovering the SUAS, changing its battery, pre-flight procedures, and re-launching. To safeguard the qualities of the small UAV, it has not been possible to broaden the flight endurance by adding more batteries; therefore, the best option to supplement the onboard battery supply to extend the flight endurance is to utilize lightweight photovoltaic (PV) cells.

B. SUAS CAPABILITIES AND MISSIONS

Utilizing SUAS improves military units' situational awareness with the end goal of avoiding putting lives in harm's way. One of the key points of having SUAS within military organizations is that the aircraft are easily assembled and portable for military unit of any size, which means that SUAS can be launched on demand without the need for a formal request for a higher reconnaissance asset. The UAS overhead essentially augments the visual scope ahead of the military unit, providing the unit time to make good decisions. This provides that military unit an advantage of conducting its own reconnaissance and enhancing its members' situational awareness on the terrain and possible threats.

The use of SUAS has become an essential piece of equipment for any military unit, whether on the ground or at sea. There are still a few restrictions on the ability of the SUAS used for ISR missions. Essentially, the flight endurance and the amount of time to re-launch the recover aircraft are concerns. Most small military units only have one or two SUAS, and with their short flight endurance, it is hard for the unit to take full advantage of its ISR capability. One approach is to expand the flight endurance of the SUAS. Expanded perseverance permits continuous ISR coverage over its area. The main advantage of extending the flight time is that a military unit only needs one aircraft and, possibly, only one battery, without sacrificing the aerial coverage.

C. OBJECTIVE

To broaden the flight continuance of a SUAS, in this research we concentrate on utilizing thin film photovoltaic (TFPV) cells to supplement the battery source. TFPV cells are lightweight, durable, and flexible. This makes TFPV cells the best option to integrate onto SUAS to supplement the onboard battery source. Augmenting the battery supply with TFPV cells can provide two benefits: 1) expanded flight continuance 2) and the capability to re-charge the battery while in flight. This project utilizes a platform that has not previously been used with solar cells but is more commonly used in the military today. The Puma RQ-20B Digital Data Link (DDL) fills in as the test platform to demonstrate the attainability of expanding the flight continuance of military SUAS. We

assess the feasibility of augmenting the battery source with the TFPV integration by experimental testing and simulated flight test.

Another imperative question this proposal addresses is the means by which this procedure can be made cost effective by utilizing widely available commercial products to integrate solar cells that either match or exceed the power consumption of the aircraft.

D. APPROACH

In this thesis, we explore the suitability of the new TFPV cells with a higher efficiency. The goal is to maximize the output power of the new TFPV cells and determine their actual output and efficiency. The intent is to maximize the exposure to available solar irradiance given the area of the wing by designing and modifying a solar array utilizing the new TFPV cells. The solar array effectiveness is subjected to final simulation and testing prior to mounting on the Puma UAV wing. This determines if the given area and TFPV cells are sufficient to augment the power supply of the Puma while in operation.

II. FUNDAMENTALS

In this chapter, we focus on providing a concise outline of operational SUAS, photovoltaic cells basics, and past projects at the Naval Postgraduate School (NPS) concerning SUAS and solar cells. Previous projects have demonstrated the plausibility of increasing the flight endurance of SUAS [2], [3]. Expanding on previous research on the integration of solar cells on SUAS, we demonstrate the expanded ability on a larger platform using high efficiency thin film photovoltaic (TFPV) cells as the prime choice to satisfy the objective of this research.

A. UNMANNED AERIAL VEHICLES

UAVs have been used by all branches of the U.S. military, particularly for ISR missions. ISR missions include surveying and transmit vital data information back to the military unit. These missions typically require the UAV to be deployed ahead of the unit and to conduct its ISR mission for as long as its battery permits.

The United States Military utilizes an extensive variety of UAVs, whether electric or fossil fuel propulsion. In this section, we review the distinctive sorts of UAVs used today, in particular the Puma RQ-20B, Raven RQ-11B, Wasp RQ-12A, and Desert Hawk [4]. The key aim is to distinguish their framework capacities and the significance of utilizing their vast wings' surface area for solar cell applications. The Department of Defense categorizes UAVs by their operational capability [4], as shown in Table 2.

Table 2. UAV Classifications. Source: [4].

UAS Category	Speed (knots)	Weight (lbs)	Operating Altitude (ft)	Aircraft Examples	Inventory as of 1 July 2013
Group 1	< 100	0-20	< 1,200 AGL	Puma, Raven, Wasp, T-Hawk	9,765
Group 2	< 250	21-55	< 3,500 AGL	ScanEagle	206
Group 3	< 250	< 1320	< 18,000 MSL	STUS, Shadow EUAS	537
Group 4	Any	> 1320	< 18,000 MSL	Predator, Hunter, Gray Eagle, Fire Scout	309
Group 5	Any	> 1320	> 18,000 MSL	Reaper, Global Hawk	147

In this research, we focus on Group 1 platforms, which are all battery operated, making their flight endurance limited in comparison to the other groups. As the demand for real-time reconnaissance increases, it is vital that we continue to explore new technologies to extend the endurance of Group 1 platforms. In this research, we demonstrate the feasibility of improving the flight endurance of Group 1 fixed-wing platforms.

1. PUMA AE (RQ-20B)

According to the AeroVironment website [5], the Puma All Environment (AE) is a completely waterproof unmanned aircraft intended for both land and sea operations. The website further explains: “Capable of landing in water or on land, the Puma AE empowers the operator with an operational flexibility never before available in the small UAS class” [5]. The operator is able to control the Puma manually or use the GPS autonomous navigation via the Ground Control Station (GCS). The Puma UAV is a lightweight, portable system that can be launched by a single person, and with its aerodynamic design it provides an increased payload and stability, as shown in Figure 1 [5].

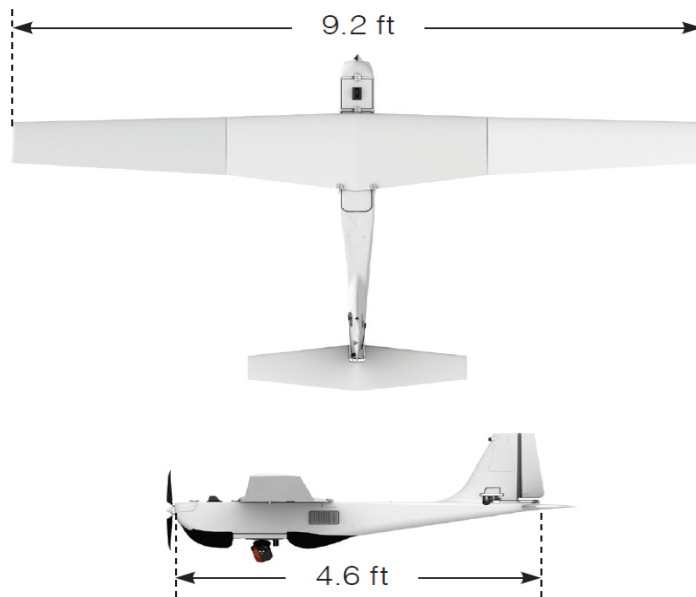


Figure 1. Puma AE (RQ-20B). Source: [5].

A brief overview of the Puma's UAS specifications and capabilities is given in Table 3. With its wing surface area, the Puma is suitable for solar cells integration. The wing surface area alone is large enough to incorporate a large number of TFPV cells. The U.S. Marine Corps [6] and Army [7] continue to procure more Pumas, while the U.S. Navy is deploying and testing the Puma capabilities on destroyers and patrol craft in the Persian Gulf [8]. As the U.S. military continues to expand its Puma fleet, due to its increased capability from previous platforms, the Puma was chosen as the test platform and provides ample wing surface area for solar cell integration. Moreover, we obtained a full set Puma AE (RQ-20B) wing from Evolving Resources Incorporated (ERI), which is the depot the U.S. Army, Marine Corps, and Navy use to upgrade and repair their SUAS. With their cooperation, we were allowed to observe while they conducted a full test and collected the data we had requested for use in this research.

The main goal of this research is to extend the flight endurance of the Puma by integrating PV cells on its wing.

Table 3. Puma AE (RQ-20B) Specifications. Source: [5].

Parameter	Specifications
Wingspan	9.2 ft (2.8 m)
Length	4.6 ft (1.4m)
Weight	14 lbs
Wingspan Area	approx. 7160 cm ²
Range	15 km
Endurance	3+ hrs
Speed	25-45 kt
Operating Altitude	500 ft AGL
Maximum Operating Altitude	12,500 ft
Ground Control Station	Common GCS
Launch Method	Hand-Launched or Rail Launch
Recovery Method	Deep Stall Landing
Payload	Gimbaled payload with EO and IR

2. RAVEN (RQ-11B)

The Raven (RQ-11B), shown in Figure 2, is smaller than the Puma platform and is strategically operated at the U.S. Army and Marine Corps battalion, company and platoon level. The Raven falls into the same group of UAVs as the Puma and utilizes the same common GCS for flight operations. Due to its small scale, it is highly man-portable and lightweight for quick deployment that provides reconnaissance, surveillance, and target acquisition (RSTA). Since it utilizes the same GCS as the Puma, the operator is able to control the Raven manually or use the GPS autonomous navigation via the hand controller or RSTA laptop.



Figure 2. Raven (RQ-11B). Source: [9].

The Raven has demonstrated its combat effectiveness in Iraq, the Afghanistan conflict, and in other missions in which we have operated since the Raven entered

service. A brief overview of the Raven's UAS specifications and capabilities is presented in Table 4.

Table 4. Raven (RQ-11B) Specifications. Source: [9].

Parameters	Specifications
Wingspan	4.5 ft (1.4 m)
Length	3.0 ft (0.9m)
Weight	4.2 lbs
Wingspan Area	approx. 2278 cm ²
Range	10 km
Endurance	60-90 mins
Speed	17-44 kt
Operating Altitude	100-500 ft AGL
Maximum Operating Altitude	14,000 ft
Ground Control Station	Common GCS
Launch Method	Hand-Launched
Recovery Method	Deep Stall Landing
Payload	Gimbaled payload with EO and IR

3. WASP AE (RQ-12A)

The Wasp is the smallest fixed-wing platform in Group 1 to be considered for this research, as shown in Figure 3. With its all-environment design for sea and land operations, the Wasp delivers a light weight, highly portable platform for rapid deployment for RSTA operations. A brief overview of the Wasp's UAS specifications and capabilities are listed in Table 5. The Wasp also uses the same GCS as the Puma and Raven, so the operator is capable of controlling the Wasp manually or using the GPS autonomous navigation via the hand controller or RSTA laptop. Because of its limited wing surface area, range, and weight carrying capability, the Wasp was not considered for solar cell integration.



Figure 3. Wasp AE (RQ-12A). Source: [10].

Table 5. Wasp AE (RQ-12A) Specifications. Source: [10].

Parameters	Specifications
Wingspan	3.3 ft (1.0 m)
Length	2.5 ft (0.762m)
Weight	2.85 lbs
Range	5 km
Endurance	50 mins
Speed	Cruise: 20 kt Dash: 45+ kt
Operating Altitude	500 ft AGL
Ground Control Station	Common GCS
Launch Method	Hand-Launched
Recovery Method	Deep Stall Landing
Payload	Gimbaled payload with EO and IR

4. DESERT HAWK III

The Desert Hawk III is an autonomous all environment SUAS for day/night operations to conduct RSTA missions. It has the capacity for quick interchangeable

payloads for mission adaptability. The U.S. Air Force has since replaced its Desert Hawk fleet for the Raven [11], but it is widely used by the British Army [12]. Due its limited availability in the U.S. UAV fleet, the Desert Hawk was not chosen for evaluation for solar integration. Desert Hawk’s specifications are shown in Table 6.

Table 6. Desert Hawk III Specifications. Adapted from [13].

Parameters	Specifications
Wingspan	4.11 ft (1.25 m)
Weight	8.2 lbs
Range	5 km
Endurance	90 mins
Speed	Cruise: 25 kt Dash: 50 kt
Ground Control Station	Autonomous GPS Nav
Launch Method	Hand-Launched
Recovery Method	Deep Stall Landing
Payload	2 lbs

In this section, we examined different available small military UAV platforms (but not all), such as the Puma, Raven, Wasp, and Desert Hawk. For each platform, we discussed capabilities, physical dimensions, and limitations. In deciding upon the ideal platform for this research, we chose a platform that has ample wing surface area, has never been researched for solar cell integration, and the military prefers because of its increased capability; the platform chosen for this research is the Puma UAV.

B. PRACTICAL SOLAR CELLS

Solar cells are simple semiconductor devices that generate electricity from visible light. They are usually constructed from materials that are either single crystal, crystalline, or amorphous semiconductors. They are composed of two types of material, a p-type material and n-type material [14]. Since solar cells are semiconductors with a p-type base and n-type emitter, light produces electron-holes on both side of the junction [14]. The solar cell surface area, solar irradiance level, and its efficiency determine the amount of energy generated.

When considering solar cells, there are some important characteristics to consider. Their output decreases about $2.0 \text{ mV}/^{\circ}\text{C}$, and the output voltage is independent of cell size [14]; however, at higher temperatures, current is relatively stable and is directly proportional to the solar irradiance and cell area [14]. To obtain its maximum output power, the solar cells must be operated at relatively low temperatures, around $25^{\circ}\text{C} \pm 15\%$ [14]. The maximum output power is also directly proportional to the solar cell material and its efficiency. The common method to analyze the effectiveness of a PV cell is to examine the current-voltage curve (IV curve), as illustrated in Figure 4. There are five parameters that define the characteristics of a solar cell: open circuit voltage (V_{OC}), short circuit current (I_{SC}), fill factor (FF), maximum power (MP), and energy conversion efficiency (η) [14].

In this section, we will discuss factors that influence solar cell efficiency and encapsulated flexible TFPV cells. This research will show the growing capability and efficiency of using TFPV cells.

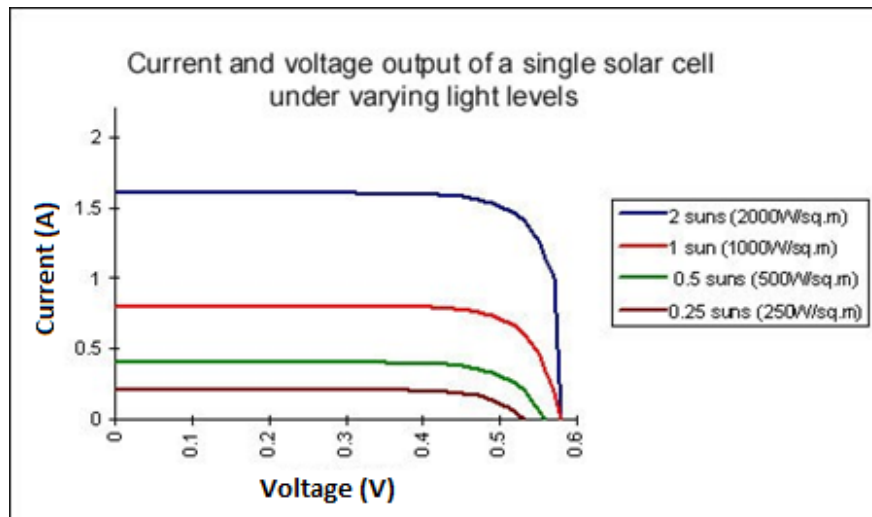


Figure 4. IV Curve Example at Different Solar Intensity. Adapted from [2].

1. FACTORS THAT INFLUENCE SOLAR EFFICIENCY

The main factors that affect solar cell efficiency are cell temperature, photovoltaic material, anti-reflection coating, and electrical resistance in metal contacts, surface, and

base. The photovoltaic material must have the capacity to retain solar irradiance. Most of the solar irradiance is absorbed on the surface, and the anti-reflection coating determines how many of the light photons are transmitted to the photovoltaic material. The photovoltaic material then converts the absorbed photons to electricity; depending on its properties, the light may be absorbed, reflected, or passed through.

The anti-reflection coating also serves another purpose—it seals the photovoltaic material from the elements and slows the cell degradation. Low energy photons create heat instead of electron-hole pairs. Similarly, photons with excess energy create electron-hole pairs, a by-product of excess heat. As stated before, output voltage decreases $2.0 \text{ mV}/^{\circ}\text{C}$; an example of how temperature affects a single solar cell is illustrated in Figure 5. Prolonged heat exposure can prematurely degrade the solar cells, resulting in the reduction in cell efficiency. Lastly, excess resistance in the metal contacts, surface, and base can further reduce the cell efficiency.

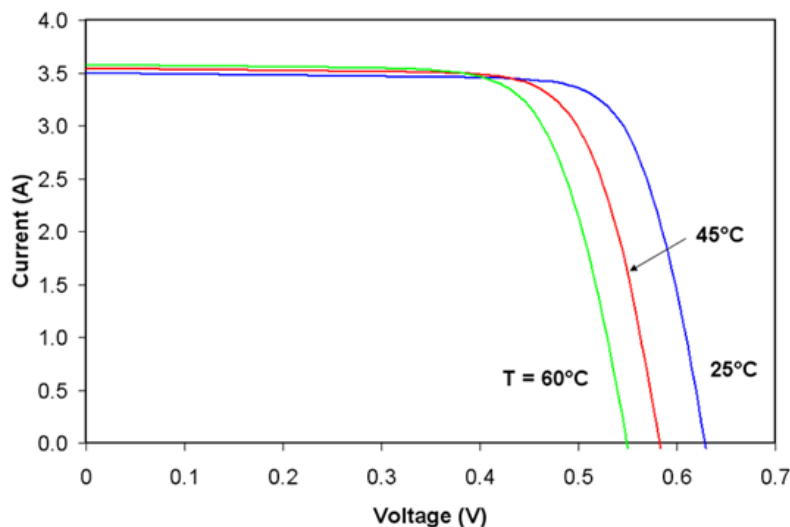


Figure 5. Example of How Temperature Affect a Single Solar Cell.
Source: [15].

As technology continues to advance and better materials are discovered for solar cells or the manufacturing process is refined, we will continue to see a rise in more efficient solar cells. As shown in Figure 6, the National Renewable Energy Laboratory

(NREL) has been tracking the evolution of solar cell efficiency since 1976 from various educational facilities as well as corporations.

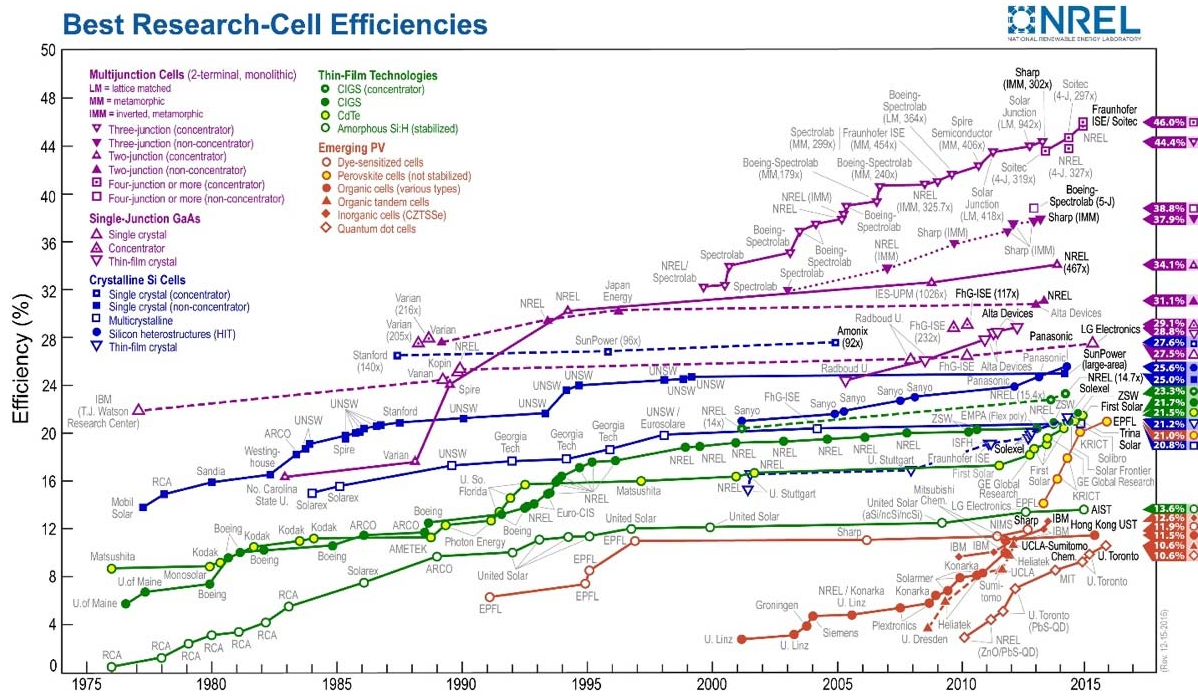


Figure 6. NREL Best Research-Cell Efficiencies, since 1976.

Source: [16].

2. ENCAPSULATED FLEXIBLE TFPV CELLS

Encapsulated flexible TFPV cells are generally composed of multiple thin layers; each layer serves a purpose. In general, there are five basic layers: conductive layer, solar irradiance absorber layer, window layer, transparent conductive oxide, and the substrate. Each of these components is comprised of different chemical and physical properties that contribute to the overall performance and efficiency of the solar cell.

The substrate provides the flexibility and durability to the solar cells. It is also the passive component in the solar cell. The conductive layer is applied to the p-type semiconductor in the substrate [14]. To have a proper contact between the conductive layer and the substrate, the resistance of the conductive layer must be greater than that of

the p-type semiconductor in the substrate [14]. Due to its relatively inert nature, molybdenum (Mo) is generally used as the contacting material in the substrate.

The transparent conductive oxides are generally the n-type semiconductors due to its electrical characteristics in the visible spectrum. With their low resistivity, this ensures that the maximum available light is transferred and absorbed by the solar irradiance absorber layer. The transparent conductive oxide conductivity is highly dependent on the carrier mobility and concentration [14].

A junction region to the solar irradiance absorber layer is formed by the window layer. This ensures the maximum available solar irradiance is admitted to the solar irradiance absorber layer. The window layer does not provide any photovoltaic generation. Cadmium sulfide (CdS) is typically used for the window layer.

In TFPV, the most common material used for the solar irradiance absorber layer is copper-indium-gallium di-selenide (CIGS). The general band-gap energy for CIGS is 1.53 eV, which makes it an ideal material for photovoltaic generation. Due to its high absorbing semiconductor properties and its ability to trap solar irradiance in the junction region, it makes an excellent choice for solar cells. A typical schematic of a CIGS TFPV cell is illustrated in Figure 7.

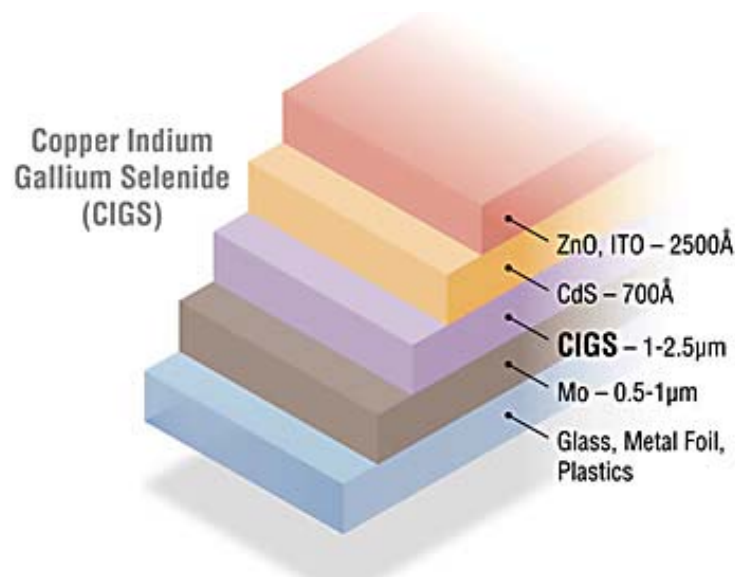


Figure 7. Schematic Illustration of a Typical CIGS Substrate. Source: [17].

THIS PAGE INTENTIONALLY LEFT BLANK

III. TFPV ON PUMA

The selected SUAS platform and PV cell are discussed in this chapter. Additionally, its design, solar cell integration, as well as system testing are presented. Some of the presented SUAS data are assumptions derived from the available information in the operational manual and the experts who repair, upgrade, and have extensive experience from testing the SUAS platform.

Before the design and integration phase, it is vital to measure the electrical characteristics of each TFPV cell submodule. This was conducted in the local climate conditions of Monterey, California. It is important to measure the electrical characteristics of each submodule to verify the manufacture's claim and to identify any defected submodules prior to integrating on the SUAS wing assembly.

A. BEST SUAS FOR SOLAR CELL INTEGRATION

With the growing demand for ISR-capable SUAS by units throughout the U.S. military, it is vital to select a platform that is widely used and has ample surface area for solar cell integration; therefore, the Puma UAV was selected for this research. The Puma has a proven track record; its all-environment platform it makes suitable for all units throughout the U.S. military. With the Marine Corps, Army and Navy acquiring and utilizing the Puma in the field, the Puma makes the best choice to examine ways to extend its flight endurance.

The Puma's Li-ion polymer battery is a sealed battery pack that utilizes a smart chip that makes it inoperable upon detection of any abnormalities to its connection, a picture of the Puma Li-ion battery pack is shown in Figure 8. Due to the characteristics of the Puma's battery and the limited availability of the Puma to test and collect electrical load, current, and power consumption at different operating throttles, best estimates on power consumption was gathered from information provided in the operating manual and experience from ERI personnel. The current endurance or operating time for the Puma is about 3 to 3 1/2 hours (or 210 minutes). Prior to operating the Puma for any flight missions, the operator must first conduct pre-flight procedures, which takes

approximately ten minutes, depending on the experience of the operator, leaving the Puma with 200 minutes of flight endurance.

The Puma's Li-ion polymer rechargeable battery pack is rated at 25.2 V and has a capacity of 13.5 A-hrs [18]. The low-voltage warning occurs at 18.8 V, or approximately 20% of the battery's current capacity, which is approximately 2.7 A-hrs, giving the aircraft 10.8 A-hrs for flight missions [18]. According to ERI's testing, the Puma uses about 10% of its current capacity for takeoff, leaving 9.72 A-hrs (or 583.2 A-mins) for flight missions. From this information, we calculate that the Puma operates at approximately 2.916 A.



Figure 8. Puma Li-ion Polymer Battery. Source: [18].

The Puma has a wingspan area of approximately 7160 cm², providing ample surface area to integrate solar cells on the wings. The Puma also represents a platform that can gain the most capability compared to the other Group 1 assets due to its available surface area. Additionally, we obtained a Puma wing assembly from ERI, allowing us to test and utilize the wing in this research, as shown in Figure 9.



Figure 9. Puma Wing

B. GLOBAL SOLAR TFPV SOLAR ARRAY

TFPV CIGS cells are a proven option for low cost, thin film solar cells and have adequate power output and efficiency. Due to its multiple layers, TFPV CIGS cells have a high tolerance to solar irradiance during extended exposure, making TFPV CIGS cells well suited for SUAS solar-cell integration; however, CIGS cells are more susceptible to the elements, which degrades efficiency over time if not encapsulated. Among other thin-film solar cells, CIGS provide the highest efficiency that is currently available in the commercial market at relatively low cost. The NREL states,

The National Center for Photovoltaics (NCPV) at NREL has significant capabilities in copper indium gallium diselenide (CIGS) thin-film photovoltaic research and device development. CIGS-based thin-film solar cell modules represent the highest-efficiency alternative for large-scale, commercial thin-film solar cells. Record small-area single-junction efficiency now tops 22% and several companies have confirmed module efficiencies exceeding 16% [17].

For this research, we decided to utilize a new commercial-off-the-shelf (COTS), high efficiency TFPV cell sub-module that incorporates CIGS cells from Global Solar. This solar submodule is flexible, durable, encapsulated, and weighs 35 grams (or 1.13 oz) for each sub-module. With an efficiency of 15%, rated maximum voltage of 6.4 V, and rated power of 8.3W, Global Solar TFPV CIGS cells make a good choice to supplement the onboard battery. At a price of \$18 per sub-module, or \$2 per W, this makes it a perfect choice for low-cost acquisition. Global Solar typical performance at a solar irradiance level 1000 W/m^2 and a cell temperature of 25°C is shown in Figure 10 [19]. A summary of Global Solar TFPV cell specifications is shown in Table 7.

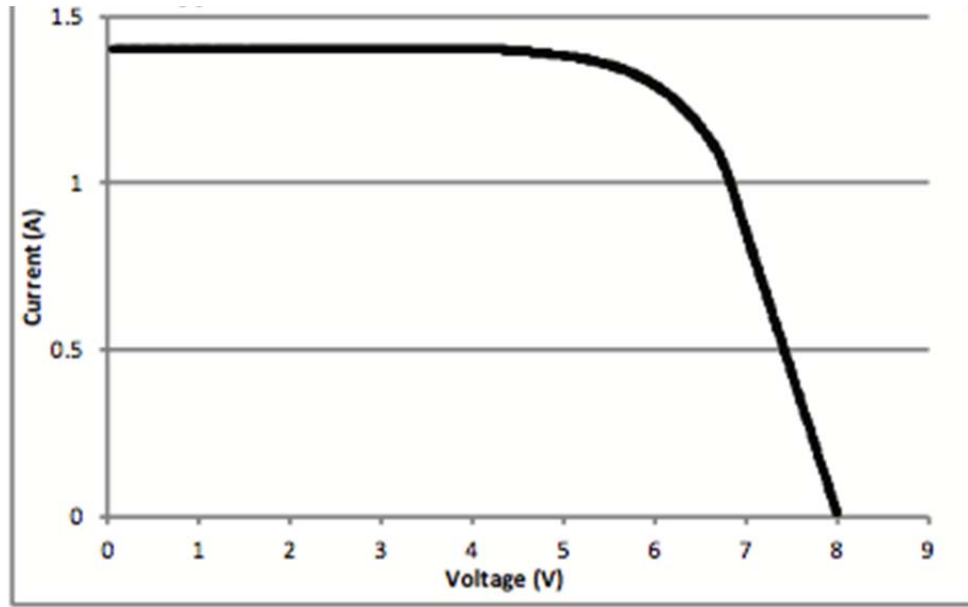


Figure 10. Global Solar FG-SM12-11 Submodule Typical Performance.
Adapted from [19].

Table 7. Global Solar FG-SM12-11 TFPV Cell Specifications.
Adapted from [19].

Product Specifications	Value
Rated Power	8.3 W
Rated Maximum Voltage	6.4 V
Rated Maximum Current	1.3 A
Open Circuit Voltage	8.0 V
Short Circuit Current	1.4 A
Efficiency	15%
Overall Dimensions	230 × 294 × 0.29 mm
Cell Array Aperture	220 × 261 mm
Cell Array Area	574 cm ²
Weight	1.13 oz

The advantages of encapsulated thin film CIGS solar cells are their light weight, durability, low cost, and capability to maintain constant performance during extended solar irradiance exposure. Combination with a DC-to-DC converter further enhances the PV array application.

IV. EXPERIMENTAL RESULTS

In this chapter, we focus on the solar power output and the arrangement of TFPV CIGS cells on the Puma wing. With the information on the Puma's power consumption from the previous chapter, we can theoretically estimate its flight capabilities and limitations of the selected solar cell to integrate on the Puma. First, IV curves are plotted for a single TFPV submodule, the left TFPV solar array, the right TFPV solar array, and finally, the left and right TFPV solar array in parallel.

A. FG-SM12-11 SOLAR MODULE TESTING

To better gauge the capability of the solar cell chosen, several experimental tests were conducted to determine the power output. To determine the power output, we measured the electrical characteristics and solar efficiency. From the measured electrical characteristics, we determined the method of the solar structure to integrate the TFPV array with the AV power supply.

The first step in analyzing the capability of a single submodule TFPV cell is to determine the IV characteristics. The average electrical characteristics are shown in Table 8. Utilizing the Amprobe SOLAR-600 Power Analyzer, we measured the average IV and power curve of the TFPV cell at a maximum solar power of 1012 W/m^2 , illustrated in Figure 11.

Table 8. Electrical Characteristics of a Single TFPV Submodule

Parameter	Value
V_{OC}	7.862 V
I_{SC}	1.548 A
V_{MP}	6.166 V
I_{MP}	1.332 A
P_{Max}	8.213 W

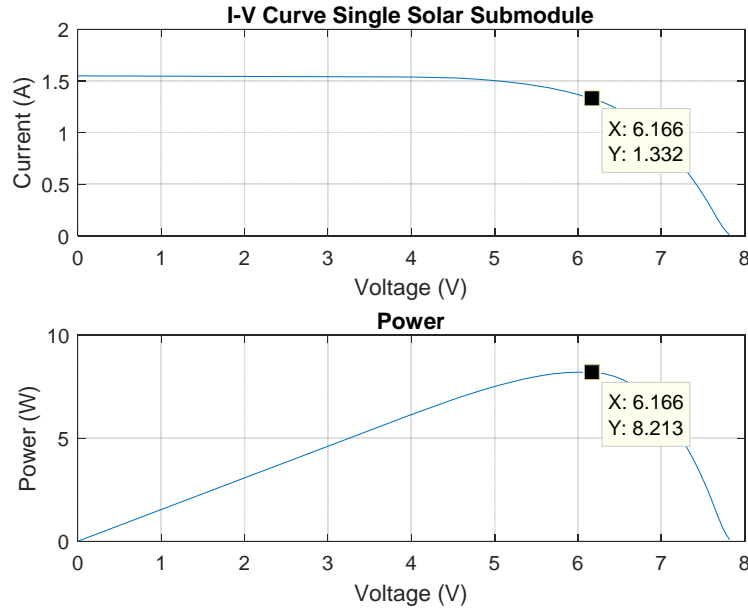


Figure 11. Average IV and Power Curve of a Single TFPV Submodule

The TFPV cell was tested under ideal sunny conditions in Monterey, California. The manufacturer's Standard Test Conditions (STC) are defined for a solar irradiance of 1000 W/m^2 under spectrum air mass (AM) 1.5 at 25°C . The maximum power point produced by the solar submodule can be determined from the IV curve. The IV curve measured in Monterey is on par or exceeds some parameters of the STC. The results measured from the single TFPV submodule are very promising.

B. LEFT AND RIGHT TFPV SOLAR ARRAY

Prior to constructing the left or right solar array, we tested and matched each of the submodule IV characteristics to get the best results upon combining the submodules. Due to the inclement weather during the testing, we utilized the solar simulator to closely simulate the test environment from the previous test. The output power of the solar simulator (approximately 750 W/m^2) was unable to recreate the same solar irradiance as the previous testing, but by having the solar simulator radiate a constant solar irradiance level, we were able to compare each submodule against each other and group comparable submodules in accordance with their electrical characteristics. In the experiment, fourteen TFPV submodules were purchased and tested. Based on the power supplied by the

battery and the power consumption of the AV, the solar design requires two separate PV submodules to be wired in series, and then connected in parallel. It is important to eliminate any defective submodules and choose the highest-quality submodules to incorporate into the final design. Each submodule array must be wired in series in order to gain a sufficient voltage to operate the AV and both arrays must be wired in parallel to satisfy the current draw.

After separating the left and right solar submodule arrays, each TFPV submodule was trimmed of excess encapsulation film. This served two purposes: first, the weight of each solar submodule was reduced to approximately 0.91 oz; second, this provided ease of access to the solar module conductive contacts. Images of the excess encapsulation film before and after trimming are shown in Figure 12.

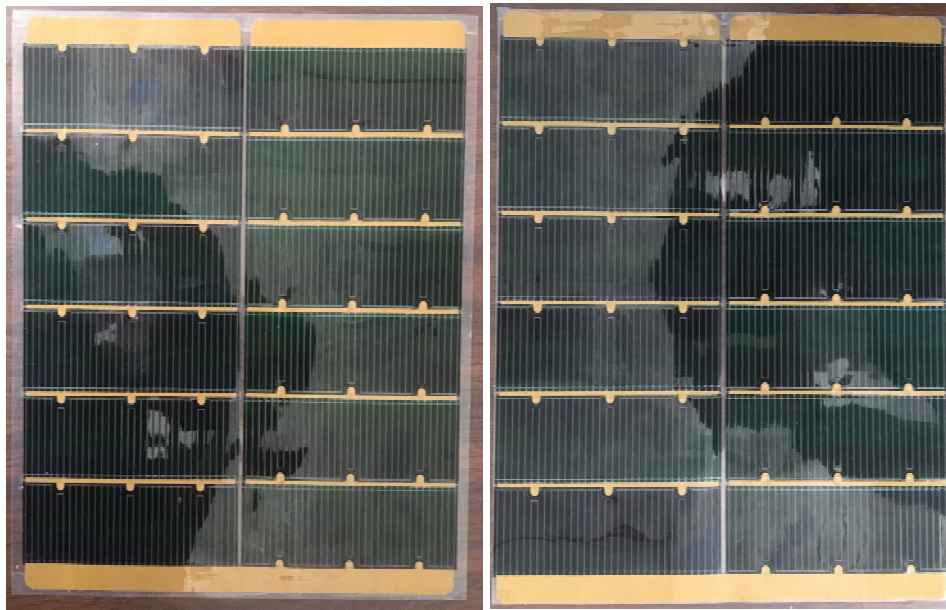


Figure 12. Un-Trimmed Submodule (left), and Trimmed Submodule (right)

From the available wing surface area, we were able to construct five submodules in series for the left and right sections of the wing, respectively. The left and right solar arrays were tested under ideal solar irradiance conditions, with a maximum solar power of 1030 W/m^2 . Utilizing the Amprobe SOLAR-600 Power Analyzer, we were able to conduct multiple measurements to obtain the average IV and power curve of the TFPV

arrays, as illustrated in Figure 13. The average electrical characteristics are shown in Table 9.

Table 9. Left and Right Solar Array Electrical Characteristics

Parameter	Left Array	Right Array
V_{OC}	38.876 V	38.821 V
I_{SC}	1.549 A	1.534 A
V_{MP}	30.588 V	30.563 V
I_{MP}	1.384 A	1.369 A
P_{Max}	42.322 W	41.829 W

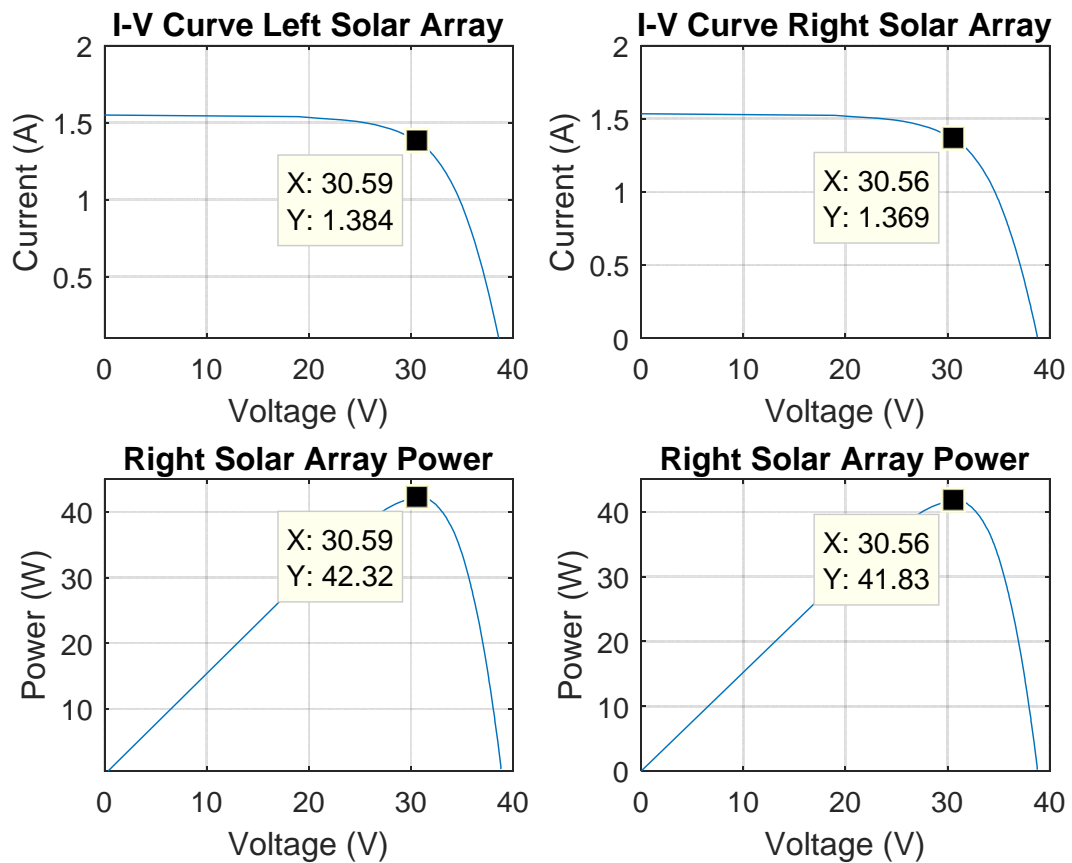


Figure 13. Average IV and Power Curve for Left and Right Array

C. FULL SOLAR ARRAY

In the final construction of the PV array, the modularity of the Puma wing was not maintained to simplify the integration between the two solar arrays; however, we were able to maintain the three wing sections for ease of disassembly by utilizing $5.5\text{mm} \times 2.1\text{mm}$ male and female DC power supply connectors, as shown in Figure 14. One of the main benefits of using TFPV cells is their flexibility, which allows the submodules to conform to the aerodynamics of the wing.

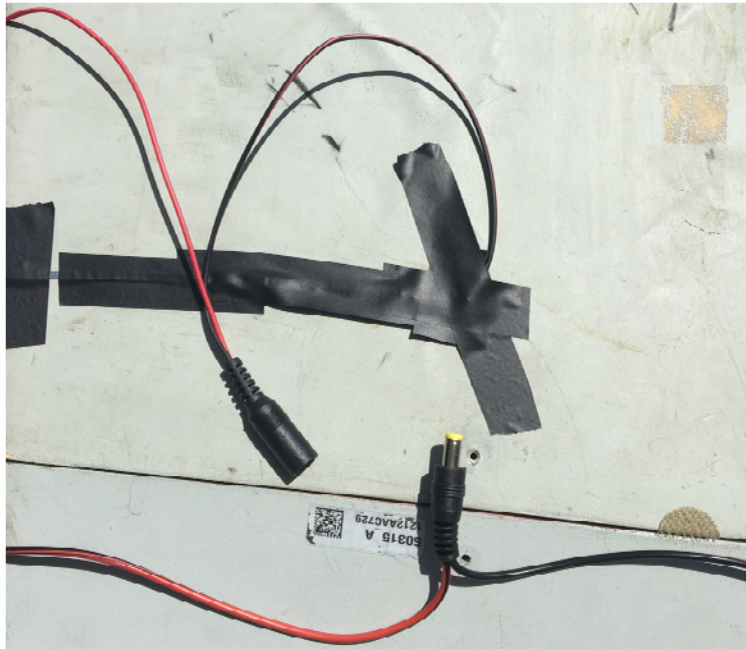


Figure 14. Male and Female DC Power Supply Connectors

Once each solar array was tested to ensure electrical conductivity, the solar arrays were connected in parallel via the DC power supply connectors. The fully assembled wing with the solar arrays is shown in Figure 15. The fully assembled wing was too large to utilize the solar simulator. Luckily, the weather conditions used to test each solar array held throughout the week. Under the same weather conditions, we were able to obtain the desired electrical characteristics. The electrical characteristics of the solar arrays connected in parallel are shown in Table 10. The IV and power curve for the fully assembled solar arrays are illustrated in Figure 16.



Figure 15. Fully Assembled Wing with the Solar Arrays

Table 10. Combined Solar Electrical Characteristics

Parameters	Value
V_{OC}	39.114 V
I_{SC}	2.985 A
V_{MP}	30.684 V
I_{MP}	2.661 A
P_{Max}	81.662 W

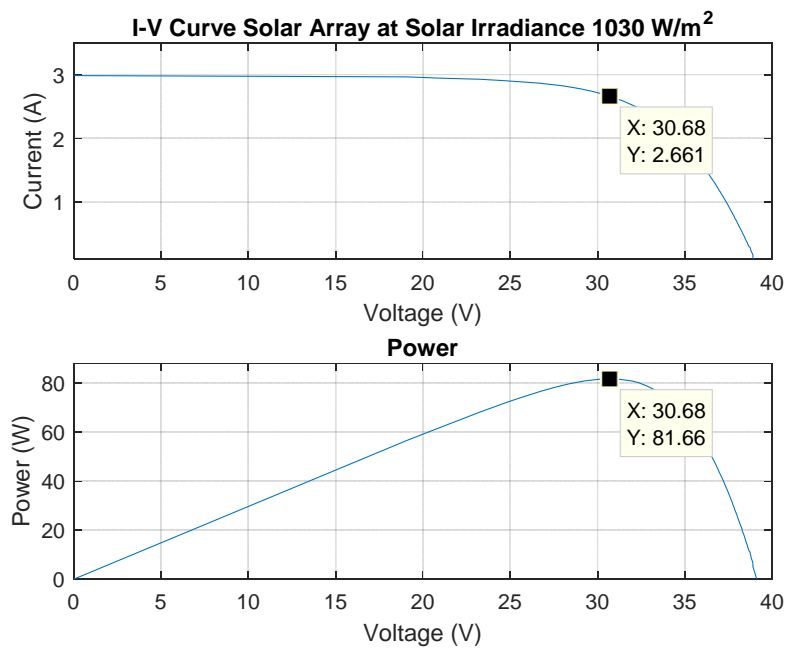


Figure 16. Average IV and Power Curve for Combined Solar Arrays

D. PV EFFICIENCY AND FILL FACTOR

To properly evaluate the effectiveness of the PV cell, we analyzed its electric characteristics. The common method uses its efficiency n [14]

$$n = \frac{P_{out}}{P_{in}} 100\% = \frac{P_{out}}{EA} 100\% \quad (1)$$

The efficiency is the ratio of the electrical output power P_{out} (in W) to the incident power (or input power P_{in}), which is in the form of solar irradiance E (in W/m²) multiplied by the surface area A (in m²) of the PV cell [14]. When we tested each individual TFPV submodule for its efficiency, we got an average efficiency of 13.8%.

Another important parameter for analyzing the effectiveness of the PV cell is the fill factor FF , which is used to determine solar cell performance. The FF is a comparison of the measured maximum power point to the theoretical power [14]:

$$FF = \frac{P_{max}}{V_{oc}I_{sc}} 100\% \quad (2)$$

The theoretical power is calculated from the open circuit voltage V_{oc} and the short circuit current I_{sc} . The closer the fill factor is to 100%, the higher the quality of the solar cell [14]. Most of the submodules used had FF s between 70 and 72%. When testing the individual submodules, we ensured that none used in the solar array had FF s that were less than 70%.

Theoretically, 5,740 cm² can be covered with ten TFPV submodules or 120 TFPV cells producing approximately 82 W. Using the maximum power point, we theoretically expect approximately 31 V and 2.65 A. The Puma wing has a surface area of 7,160 cm², but we can only cover 80.2% of the wing surface area. If we further reduce the excess encapsulated film and conductive contact material, we can better optimize the design. This can be achieved through professional manufacturing that can refine the assembly process and by adding more cells through customization.

E. SUMMARY

Due to the availability and our limited access to the Puma UAV, theoretical assumptions for the Puma power consumption is gathered through the operational manual and ERI's operating experience. From these assumptions, we determined the average power consumed by the Puma during flight was 73.5 W at a rated current of 2.916 A. With the PV array, we achieved an efficiency of 13.8% that produces a maximum power output of 81.7 W at a rated current of 2.7 A. With the current design, we can theoretically extend the flight duration of the Puma indefinitely in daylight operations under ideal solar conditions. We conclude that the integration of CIGS TFPV cells theoretically exceeds the power and current consumption of the AV vehicle, both powering the AV vehicle and recharging the onboard battery.

V. CONCLUSION AND RECOMMENDATIONS

A. SUMMARY

In this research, we explored current SUAS used by the military, including their capabilities, advantages, and limitations. With the growing use and popularity of SUAS among each of the military services, SUAS provides the user rapid deployment capability from a safe distance for ISR missions that provide the unit leader real-time information. With the need to provide the warfighter the best capable AV, the demand to increase flight endurance is a must for a wide range of missions.

The goal of this research was to establish the ground work for integrating low-cost and high efficiency TFPV cells to augment the AV onboard battery supply in order to extend the flight endurance. One of the major contributions to this research was to obtain the Puma wing and the operational manual. The Puma wing provided us the platform to integrate and test the PV arrays. The operational manual provided the baseline for the Puma's power and current consumption. With the information provided by the operating manual and ERI, we were able to theoretically estimate the average power and current consumption of the Puma, 73.5 W at a rated current of 2.9 A.

Utilizing the TFPV submodules for the solar array design, we were able to produce a maximum power point of 81.7 W at a rated current of 2.7 A. With the current design, we can theoretically extend the flight duration of the Puma indefinitely in daylight operations under ideal solar conditions, preserving the onboard battery for night operations.

In conclusion, we successfully demonstrated the feasibility of integrating encapsulated TFPV cells to significantly extend the endurance of the Puma during daytime missions. The design illustrates the flexibility to contour to the surface of the wing, minimizing the solar array footprint while having the durability to withstand the rigors of recovering and transporting the AV. Finally, at \$2 per W, it is the most cost effective way of augmenting the AV onboard battery supply.

B. FUTURE WORK

1. Obtaining the Full Puma AV for Testing

One of the major drawbacks in this research was estimating the baseline power consumption during typical flight operations. If we utilize the RQ-20B Puma AE as the test platform, we can determine how the AV is typically controlled and operated during flight. By conducting multiple in-flight or static tests, we can determine the power and current consumption by the AV during takeoff and flight. By analyzing the throttle percentage and current draw of the motor, we gain a better understanding of what is required to augment the AV onboard battery supply.

2. Testing Other Group 1 AVs with TFPV cells

The Puma is the largest platform of the Group 1 AVs, translating to a bigger motor and weight of the platform compared to other Group 1 assets, which results in more power consumption. By incorporating these lightweight and high efficiency TFPV cells into the other Group 1 AVs, we can provide an increased capability to their flight endurance. The RQ-11B Raven has half the available wing surface area for PV array integration as the Puma. Previous research has shown that the Raven consumes an average of 51.3 W [3]. With the right design, it is feasible to increase flight endurance with these high efficiency, modular, and durable TFPV cells.

3. Utilize MPPTs in Design

The Puma wing is comprised of three sections: center, left, and right. The left and right wing sections are installed at angle of approximately 16° . As the sun hits the AV wing, the solar irradiance output is not the same throughout the TFPV cells due to the angle of the wing tips. This can be offset by utilizing multiple MPPTs in the design to optimize the power output of the wing. Furthermore, flight maneuvers cause an uneven solar irradiance distribution on the wing. By adding three MPPTs to the design, one for each section of the wing, we can mitigate the effect of the uneven solar irradiance on the wing and provide a constant power at the maximum power point.

4. Further Study of the Puma's Smart Battery

One of the challenges in obtaining the power and current consumption in the Puma AV is the accessibility of its smart battery. Due to the Puma's all-environment design, the Puma's Li-ion polymer battery is a sealed battery pack that utilizes a smart chip that makes it inoperable upon detection of any abnormalities in its connection. The operational manual is not informative with regard to how the smart battery operates, or its fault codes. With further research, knowledge of the battery's smart chip software will enable us to modify the software to accept the PV array as a battery charging medium.

5. Development of Solar Battery Charger

The characteristics of these encapsulated TFPV cells—durability, flexibility, light weight, high efficiency, and low cost—make it a prime candidate for a solar battery charger for a small unit. With the wing already constructed with PV arrays and the AV not in use, the PV array can serve as a battery charging station in the field. Battery adapters and extra electrical connectors are the only extra equipment needed. This capability gives the military unit the advantage of being able to charge batteries while the AV is not in use.

THIS PAGE INTENTIONALLY LEFT BLANK

LIST OF REFERENCES

- [1] D. Ehredt, *NATO – Joint Air Power Competence Centre, 2010–2011 UAS Yearbook – UAS: The Global Perspective*, 8th ed. Paris: Blyenburgh & Co, 2010, pp. 61. [Online]. Available: http://www.dcabr.org.br/download/eventos/eventos-realizados/2010/seminario-vant-27-10-2010/cd-uvs-yearbook/pdf/P061-062_NATO_Dave-Ehredt.pdf
- [2] C. Chin, “Extending the endurance, missions and capabilities of most UAVs, using advanced flexible/ridged solar cells and using new high power density batteries technology,” M.S. thesis, Dept. of ECE, Naval Postgraduate School, Monterey, CA, 2011.
- [3] R. Billings, “Application of interdigitated back contact silicon photovoltaic cells to extend the endurance of small unmanned aerial systems,” M.S. thesis, Dept. of ECE, Naval Postgraduate School, Monterey, CA, 2017.
- [4] *Unmanned Systems Integrated Roadmap FY 2013–2028*, DOD, Washington, DC Reference Number 14-S-0553
- [5] Puma AE RQ-20B. (n.d.). AeroVironment. [Online]. Available: https://www.avinc.com/images/uploads/product_docs/PumaAE_Datasheet_2017_Web_v1.1.pdf. Accessed Dec. 12, 2016.
- [6] *AeroVironment receives 13 Million RQ-20A Puma AE small unmanned aircraft systems order for United States Marine Corps*. (2015, Nov. 25) [Online]. Available: <http://investor.avinc.com/releasedetail.cfm?releaseid=944449>
- [7] *U.S. Army awards AeroVironment contracts totaling \$20.4 Million for RQ-20A Puma AE Unmanned Aircraft Systems sustainment*. (2015, Aug. 24) AeroVironment. [Online]. Available: http://www.avinc.com/resources/press_room/u.s._army_places_20.4_million_order_for_aerovironment_rq-20a_puma_ae_small_
- [8] *United States Navy Deploying Newly Designated RQ-20B AeroVironment Puma AE with Precision Recovery System Aboard Guided Missile Destroyer*. (2016, Aug 11) AeroVironment. [Online]. Available: <http://www.avinc.com/resources/press-releases/view/united-states-navy-deploying-newly-designated-rq-20b-aerovironment-puma-ae>
- [9] Raven RQ-11A/B. (n.d.). AeroVironment. [Online]. Available: https://www.avinc.com/images/uploads/product_docs/Raven_Datasheet_2017_Web_v1.pdf. Accessed Dec. 12, 2016.

- [10] Wasp RQ-12A. (n.d.). AeroVironment. [Online]. Available: https://www.avinc.com/images/uploads/product_docs/Wasp_Datasheet_2017_Web_v1.pdf. Accessed Dec. 12, 2016.
- [11] *U.S. Air Force Fact Sheet. RQ-11B Raven System.* (2009, Nov.) AeroVironment. [Online]. Available: https://www.avinc.com/images/uploads/product_docs/USAF_Raven_FactSheet_2.pdf
- [12] Desert hawk III. (n.d.). Lockheed Martin. [Online]. Available: <http://www.lockheedmartin.com/us/products/desert-hawk.html>. Accessed Dec. 19, 2016.
- [13] Desert hawk III. (n.d.). Lockheed Martin. [Online]. Available: http://www.lockheedmartin.com/content/dam/lockheed/data/ms2/documents/Desert_Hawk_Brochure.pdf. Accessed Dec. 19, 2016.
- [14] “Solar energy and application.” (Winter 2016). Class notes for Renewable Energy at Military Bases and for the Warfighter, Naval Postgraduate School, Monterey, CA.
- [15] *5 Factors that Affect Solar Panel Efficiency.* (2015, Jul. 20) Revolve Solar. [Online]. Available: <https://www.revovesolar.com/5-factors-that-affect-solar-panel-efficiency/>
- [16] Mathias. (2013, Aug. 29). *NREL sets new world record with two-junction solar cell.* [Online]. Available: <https://www.nrel.gov/pv/assets/images/efficiency-chart.png>
- [17] *Copper Indium Gallium Diselenide Solar Cells.* NREL. [Online]. Available: <https://www.nrel.gov/pv/copper-indium-gallium-diselenide-solar-cells.html>. Accessed Jan. 5, 2017.
- [18] *Small Unmanned Aircraft System, Puma AE II with Digital Data Link Operator's Manual,* DOD, Washington, DC, Reference Number 74186_11, 2015.
- [19] FG-SM12-11: 8.3 watt (6V) solar submodule. (n.d.). Global Solar. [Online]. Available: <http://www.globalsolar.com/sites/default/files/uploads/documents/Copy%20of%20FG-SM12-11%208.3W%20%286V%29%20Solar%20Submodule%20Data%20Sheet%20%28PROD%20LIT%20-%201000632%20-%201%20-%20B%29.PDF>. Accessed Jan. 15, 2017.

INITIAL DISTRIBUTION LIST

1. Defense Technical Information Center
Ft. Belvoir, Virginia
2. Dudley Knox Library
Naval Postgraduate School
Monterey, California